cell division (RND) efflux pumps, such as MexAB-OprM, can contribute to multiple-drug resistance.[13] Although efflux pumps have been shown to exist in *P. putida*, their role in clinical isolates of this species has been unclear due to a lack of data.

Therefore we conducted the present study with the aim of supplementing our knowledge in this regard, since more data is needed to assess the risks stemming from the increasing antibiotic resistance of *P. putida*.[14–16] In this study, we examined the genetic mechanisms of carbapenem and fluoroquinolone resistance in clinical isolates of *P. putida* obtained from the University of Tokyo Hospital.

Materials and methods

Bacterial strains

The bacterial strains used in this study were 27 clinical isolates of *P. putida* (consisting of 11 carbapenem- and ciprofloxacin (CIP)-resistant strains, 13 carbapenem-resistant and CIP-susceptible strains, and 3 carbapenem- and CIP-susceptible strains) recovered from different patients at the University of Tokyo Hospital, from November 2002 through to September 2005. All isolates were identified by the Vitek I system (bioMerieux Japan, Tokyo), the gelatin hydrolysis test, and the acylamidase test. Bacteria were stored at –80°C in trypticase soy broth (TSB, Becton Dickinson, Franklin Lakes, NJ, USA) containing 20% glycerol. Subsequently, bacteria were inoculated on Trypticase Soy Agar (Becton Dickinson) and incubated at 37°C overnight.

Antimicrobial agents

The antimicrobial agents used for susceptibility testing were as follows: imipenem (IPM, Banyu Pharmaceutical, Tokyo, Japan); meropenem (MEM, Dainippon Sumitomo Pharmaceutical, Osaka, Japan); doripenem (DRM, Shionogi Pharmaceutical, Osaka, Japan); tetracycline (TET, Pola Pharma, Tokyo, Japan); chloramphenicol (CHL, Sankyo, Tokyo, Japan); ciprofloxacin and amikacin (CIP, AMK, Meiji Seika Kaisha, Tokyo, Japan); ceftazidime (CAZ, Nippon–Glaxo-SmithKline, Tokyo, Japan); aztreonam (ATM, Eisai, Tokyo, Japan); piperacillin (PIPC, Toyama Chemical, Tokyo, Japan).

Susceptibility testing

Susceptibility testing was carried out using the broth microdilution method as described by the Clinical and Laboratory Standards Institute (CLSI)[17] with Mueller Hinton broth (MHB, Becton Dickinson). Quality control for the minimal inhibitory concentrations (MICs) was performed using the following reference strains: *Staphylococcus aureus* ATCC 21293, *Escherichia coli* ATCC 25922, and *Pseudomonas aeruginosa* ATCC 27853. Susceptibility break-points were defined according to CLSI recommendations.

Pulsed-field gel electrophoresis (PFGE)

Pulsed-field gel electrophoresis (PFGE) was carried out after digestion of the bacterial DNA with 20 U of the restriction endonuclease *Spe*I (New England Biolabs, Ipswich, MA, USA) in 1% pulsed field certified agarose (Bio-Rad, Tokyo, Japan) in 0.5×tris-borate+EDTA (TBE) buffer with a CHEF-DR II apparatus (Bio-Rad) for the analysis of genomic DNA macrorestriction patterns. BioNumerics software (version 4.0, Applied Maths, Kortrijk, Belgium) was used to analyze the DNA restriction patterns and determine their similarity, based on calculation of the Dice similarity coefficient and using the unweighted pair-group method using arithmetic averages (UPGMA) algorithm. Isolates were considered to be a cluster if the similarity value was more than 0.80.

Detection of MBL and integrase genes

Detection of MBL and integrase genes was performed by polymerase chain reaction (PCR) amplification. Genomic DNA of *P. putida* isolates was extracted as previously described.[4] PCR amplification for MBL (bla_{IMP-1}, bla_{IMP-2}, bla_{VIM-1}, and bla_{VIM-2}) and integrase (*intI-1* and *intI-3*) genes was performed with specific primer sets according to a method described previously (Table 1),[7] and was carried out using Premix *Taq* enzyme (Takara Bio, Shiga, Japan) according to the manufacturer's instructions.

Analysis of *oprD* gene expression by RT–PCR

The transcription of the porin gene (*oprD*) was analyzed with reverse transcriptase–PCR (RT–PCR). Mid-logarithmic phase cultures in TSB were pelleted by centrifugation at 13 000 g, and RNA was isolated using ISOGEN (Nippon Gene, Tokyo, Japan) according to the manufacturer's instructions. Total RNA, 1 μg, was reverse transcribed into single-stranded cDNA using a SuperScript III First-Strand Synthesis Supermix Kit (Invitrogen, Carlsbad, CA, USA) according to the manufacturer's instructions. PCR amplification of cDNA was performed using *oprD* gene-specific primer sets designed using the primer3 program available at http://frodo.wi.mit.edu/cgi-bin/primer3/primer3_www.cgi. The number of PCR cycles used came within the linearity range for PCR amplification, and constitutive expression of 16S rRNA assessed from the same cDNA preparation was used as a standard. Ten-microliter samples of each PCR product were separated by electrophoresis in 2.0% agarose and visualized by ethidium bromide staining. This experiment was repeated at least twice. The bands of the *oprD* gene were quantitated using image-scanning software (Scion Image, Scion Corporation, MD, USA) and results were standardized with the 16S rRNA band density.

Table 1. Primer used for sequencing and RT–PCR

Study and gene	Primer name	5′-sequence-3′	Reference or GenBank accession no.
PCR of MBL and integrase genes			
bla_{IMP-1}	F1	5′-ACCGCAGCAGAGTCTTTGCC-3′	7
	R1	5′-ACAACCAGTTTTGCCTTACC-3′	
bla_{IMP-2}	F2	5′-GTTTTATGTGTATGCTTCC-3′	7
	R2	5′-AGCCTGTTCCCATGTAC-3′	
bla_{VIM-1}	F3	5′-AGTGGTGAGTATCCGACAG-3′	7
	R3	5′-ATGAAAGTGCGTGGAGAC-3′	
bla_{VIM-2}	F4	5′-ATGTTCAAACTTTTGAGTAAG-3′	7
	R4	5′-CTACTCAACGACTGAGCG-3′	
intI-1	F6	5′-GCATCCTCGGTTTTCTGG-3′	7
	R6	5′-GGTGTGGCGGGCTTCGTG-3′	
intI-3	F8	5′-ATCTGCCAAACCTGACTG-3′	7
	R8	5′-CGAATGCCCCAACAACTC-3′	
PCR and sequencing of QRDRs of *gyrA*, *gyrB*, *parC* and *parE* genes			
gyrA	gyrA-F	5′-CGGTGACGTGATCGGTAAGT-3′	NP_743923.1
	gyrA-R	5′-GAAGTGCGCATGACCAAACT-3′	
gyrB	gyrB-F	5′-TACCTGGTGGAGGGTGACTC-3′	NP_742183.1
	gyrB-R	5′-AACGCAGTTTGTCGATGTTG-3′	
parC	parC-F	5′-CGAACAGGCCTACCTCAACT-3′	NP_747015
	parC-R	5′-ATGATCCGAAGTCGTTCGC-3′	
parE	parE-F	5′-TCAAGGCCAGCAAGAAGGT-3′	NP_747018
	parE-R	5′-CTTCGTCGAGGGCGTAGTAG-3′	
RT-PCR of *oprD* gene expression			
oprD	oprD-F	5′-ACAATCAAGGCCTGGTGTTC-3′	NP_743366.1
	oprD-R	5′-GACGTCACGTTCCCATTCTT-3′	
16S rRNA	16S-F	5′-AAGCAACGCGAAGAACCTTA-3′	AE015451
	16S-R	5′-CGGACTACGATCGGTTTTGT-3′	

PCR and sequencing of QRDRs of *gyrA*, *gyrB*, *parC*, and *parE* genes

Chromosomal DNA was extracted from *P. putida* isolates as previously described.[16] The QRDRs of the *gyrA, gyrB, parC*, and *parE* genes were amplified using primers designed using the primer3 program (Table 1). Amplification was carried out using Premix *Taq* enzyme (Takara Bio) as recommended by the manufacturer with an annealing temperature of 57°C. PCR products were sequenced using a BigDye Terminator v1.1 Cycle Sequence Kit (Applied Biosystems, Foster City, CA, USA) and an automated DNA sequencing system (ABI PRISM 3130xl, Applied Biosystems). A similarity search for the amino acid sequences deduced against DDBJ/EMBL/GenBank sequence databases was conducted using the BLAST program at the DNA Databank of Japan (Shizuoka, Japan).

Effects of efflux pump inhibitor

Susceptibility testing of IPM and CIP by microbroth dilution was performed in the presence and absence of the efflux pump inhibitor (EPI), L-phenylalanine-arginine-N-naphthylamide (PAβN, Sigma-Aldrich, St. Louis, MI, USA).[18] The EPI was incorporated in MHB at a concentration of 25 mg/l. When comparing MICs in the presence and absence of the EPI, a > 2-fold decrease in MICs for each antibiotic was indicated as a significant change. This experiment was repeated at least twice.

Nucleotide sequence accession number

The partial DNA sequence of the *parC* gene in Pp12 isolates has been assigned to the DDBJ/EMBL/GenBank database under the accession number AB361291.

Results

Susceptibility testing

The results of susceptibility testing are given in Table 2. All of the 24 carbapenem-resistant strains were also resistant or intermediate-resistant to the antibiotics CAZ, ATM, and CHL. Several strains showed resistance to PIPC, AMK, and TET. Three carbapenem- and CIP-susceptible strains were susceptible to the antibiotics IPM, MEM, DRM, CIP, CAZ, AMK, and TET.

PFGE

The genetic backgrounds of 27 *P. putida* strains were analyzed by PFGE. Two carbapenem- and CIP-resistant strains (Pp7 and Pp17) showed gel patterns with a similarity of higher than 0.80 (80%). However, the other strains showed different PFGE patterns with a low similarity (data not shown).

Table 2. Profiles of *Pseudomonas putida* stains in this study

Strain	Type of genes		mRNA expression[a]		Mutations[b]		MICs (mg/L)									
	β-Lactamase	Integrase	*OprD*	Gene	GyrA	ParC	IPM	MEM	DRM	CIP	CAZ	ATM	PIPC	AMK	TET	CHL
Carbapenem and ciprofloxacin-resistant strains (n=11)																
Pp1	bla_{IMP-1}	*intl-1*	2.26		Thr83Ile	–	512	256	>256	64	>64	>64	64	>128	128	256
Pp7	bla_{IMP-1}	*intl-1, intl-3*	0.12		Thr83Ile	–	128	16	128	128	>64	32	64	>128	4	128
Pp8	bla_{IMP-1}	*intl-1, intl-3*	0.11		Thr83Ile	–	128	256	128	128	>64	32	64	>128	8	>512
Pp9	bla_{IMP-1}	*intl-1, intl-3*	0.09		Thr83Ile	–	128	32	256	128	>64	16	64	>128	4	512
Pp12	bla_{IMP-1}	*intl-1*	0.53		Thr83Ile	Ser87Leu	128	64	>256	512	>64	32	32	64	64	512
Pp14	bla_{IMP-1}	*intl-1, intl-3*	0.12		Thr83Ile	–	128	256	256	128	>64	>64	128	>128	4	512
Pp16	bla_{IMP-1}	*intl-1, intl-3*	0.49		Thr83Ile	–	64	64	128	64	>64	32	32	>128	2	512
Pp17	bla_{IMP-1}	*intl-1, intl-3*	0.08		Thr83Ile	–	64	32	128	64	>64	16	16	>128	4	128
Pp18	bla_{IMP-1}	*intl-1*	0.04		Thr83Ile	–	64	128	256	512	>64	>64	>256	16	32	512
Pp22	bla_{IMP-1}	*intl-1, intl-3*	0.10		Thr83Ile	–	32	256	64	128	>64	32	32	>128	8	512
Pp24	bla_{IMP-1}	*intl-1, intl-3*	0.44		Thr83Ile	–	16	128	128	64	>64	32	32	>128	2	512
Carbapenem-resistant and ciprofloxacin-susceptible strains (n=13)																
Pp2	bla_{IMP-1}	*intl-1*	0.23		–	–	512	256	>256	<=0.5	>64	>64	64	32	32	512
Pp3	bla_{IMP-1}	*intl-1*	1.77		–	–	256	64	256	<=0.5	>64	32	32	<=2	2	128
Pp4	bla_{IMP-1}	*intl-1*	0.39		–	–	256	32	>256	<=0.5	>64	>64	16	16	4	128
Pp5	bla_{IMP-1}	*intl-1*	1.26		–	–	256	32	>256	<=0.5	>64	32	32	32	2	256
Pp6	bla_{IMP-1}	*intl-1*	0.07		–	–	128	128	256	<=0.5	>64	>64	32	<=2	16	512
Pp10	bla_{IMP-1}	*intl-1*	0.86		–	–	128	64	256	<=0.5	>64	32	16	64	4	128
Pp11	bla_{IMP-1}	*intl-1*	0.10		–	–	128	32	256	<=0.5	>64	32	32	>128	8	>512
Pp13	bla_{IMP-1}	*intl-1*	0.34		–	–	128	64	>256	<=0.5	>64	>64	>256	>128	64	>512
Pp15	bla_{IMP-1}	*intl-1*	0.36		–	–	128	64	256	<=0.5	>64	16	16	16	8	256
Pp19	bla_{IMP-1}	*intl-1*	0.11		–	–	64	128	256	<=0.5	>64	32	16	>128	8	>512
Pp20	bla_{IMP-1}	*intl-1*	0.44		–	–	64	32	256	<=0.5	>64	>64	32	64	8	256
Pp21	bla_{IMP-1}	*intl-1*	0.32		–	–	64	32	256	<=0.5	>64	32	16	16	8	256
Pp23	bla_{IMP-1}	*intl-1*	0.52		–	–	32	128	64	<=0.5	>64	16	64	4	2	256
Carbapenem and ciprofloxacin-susceptible strains																
Pp1487	ND	ND	0.84		–	–	2	4	2	<=0.5	<=1	16	16	<=2	0.5	8
Pp928	ND	ND	0.90		–	–	1	4	2	<=0.5	<=1	16	8	<=2	0.5	32
Pp1035	ND	ND	1.00		–	–	1	1	<=0.5	<=0.5	<=1	32	<=4	<=2	1	4

IPM, imipenem; MEM, meropenem; DRM, doripenem; CIP, ciprofloxacin; CAZ, ceftazidime; AMK, amikacin; ATM, aztreonam; PIPC, piperacillin; TET, tetracycline; CHL, chloramphenicol; ND, not detected

[a]The bands of the *oprD* gene by RT–PCR were quantitated using image-scanning software, and the results were standardized with the 16S rRNA band density

[b]Amino acid mutations were identified compared with the sequences of *P. putida* KT2440. –, no amino acid mutations

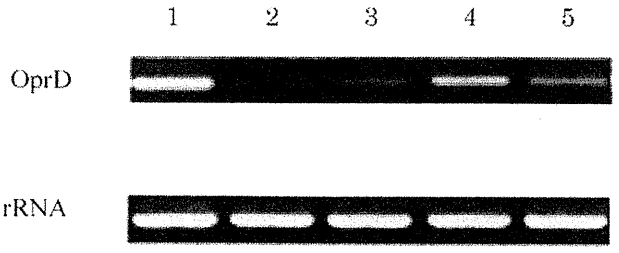

Fig. 1. Expression of *oprD* gene and 16S rRNA in clinical isolates of *P. putida* was analyzed with RT–PCR. Lanes 1 and 2, carbapenem- and ciprofloxacin-resistant strains (Pp1, 7; IMP MIC of 512, 128 mg/l); lanes 3 and 4, carbapenem-resistant and ciprofloxacin-susceptible strains (Pp2, 3; IMP MIC of 512, 256 mg/l); lane 5, carbapenem- and CIP-susceptible strains (Pp1035; IMP MIC of 1 mg/l)

MBL and integron genes

Irrespective of the levels of carbapenem resistance, all of the 24 carbapenem-resistant strains possessed bla_{IMP-1} (Table 2). The MBL genes bla_{IMP-2}, bla_{VIM-1}, and bla_{VIM-2} were not amplified by PCR. All carbapenem-resistant strains possessed *intI-1* integrase genes, and 8 carbapenem- and CIP-resistant strains had both *intI-1* and *intI-3* genes.

Analysis of *oprD* gene expression by RT–PCR

Semiquantitative analysis of *opr*D gene expression was conducted by RT–PCR. Representative electrophoresis of RT–PCR product of the *oprD* gene and 16S rRNA is shown in Fig. 1. The expression of the *oprD* gene in isolates Pp2 and Pp7 (IPM MIC of 512 and 128 mg/l, respectively) was decreased compared with that of the isolate Pp1035 (IPM MIC of 1 mg/l). On the other hand, those in isolates Pp1 and Pp3 (IPM MIC of 512 and 256 mg/l, respectively) was increased compared with Pp1035. The band density of the *oprD* gene indicated that 21 carbapenem-resistant strains were considered to have decreased expression of this gene (Table 2). The Pearson correlation coefficient (*r* value) was 0.43 for *oprD* expression levels compared with MICs for IPM, for which there was a low correlation.

Mutations in QRDRs of *gyrA*, *gyrB*, *parC*, and *parE* genes

The nucleotide sequences and derived amino acid sequences in the QRDRs of *gyrA*, *gyrB*, *parC*, and *parE* genes for each *P. putida* strain were compared with those of the control strain *P. putida* KT2440[19] (Table 2). In all of the 11 CIP-resistant strains (CIP MICs of > 64 mg/l), Thr83Ile substitutions were detected in GyrA. One strain (Pp12 having CIP MIC of 512 mg/l) had double substitutions of Thr83Ile in GyrA and Ser87Leu in ParC. None of the isolates had substitution in GyrB and ParE.

Effects of efflux pump inhibitor

The change in MIC for IPM and CIP was examined with and without the addition of EPI at a final concentration of 25 mg/l (Table 3). All of the 11 carbapenem- and CIP-resistant strains were affected by the EPI, and in 10 of them, there was a > 2-fold decrease in CIP MICs in the presence of the EPI compared with those in the absence of the EPI. In 3 strains (Pp5, Pp12, and Pp16) of the 24 carbapenem-resistant strains, there was a > 2-fold decrease in IMP MICs with the EPI as compared with those without it.

Table 3. Effects of efflux pump inhibitors in clinical isolates of *Pseudomonas putida*

Strain	MIC (mg/L)[a]			
	Ciprofloxacin		Imipenem	
	Alone	+EPI[b]	Alone	+EPI
Carbapenem and ciprofloxacin-resistant strains (n=11)				
Pp1	64	**16**	512	256
Pp7	128	**32**	128	128
Pp8	128	**32**	128	64
Pp9	128	**32**	128	64
Pp12	512	**128**	128	**8**
Pp14	128	**16**	128	64
Pp16	64	**16**	64	**16**
Pp17	64	**8**	64	32
Pp18	512	**32**	64	128
Pp22	128	64	32	32
Pp24	64	**8**	16	16
Carbapenem-resistant and ciprofloxacin-susceptible strains (n=13)				
Pp2	<=0.5	<=0.5	512	256
Pp3	<=0.5	<=0.5	256	128
Pp4	<=0.5	<=0.5	256	128
Pp5	<=0.5	<=0.5	256	**64**
Pp6	<=0.5	<=0.5	128	512
Pp10	<=0.5	<=0.5	128	256
Pp11	<=0.5	<=0.5	128	64
Pp13	<=0.5	<=0.5	128	128
Pp15	<=0.5	<=0.5	128	128
Pp19	<=0.5	<=0.5	64	64
Pp20	<=0.5	<=0.5	64	32
Pp21	<=0.5	<=0.5	64	32
Pp23	<=0.5	<=0.5	32	32
Carbapenem and ciprofloxacin-susceptible strains				
Pp1487	<=0.5	<=0.5	2	1
Pp928	<=0.5	<=0.5	1	<=0.5
Pp1035	<=0.5	<=0.5	1	<=0.5

[a] >2-fold MIC changes are in bold face
[b] Final concentration of additional EPI was 25 mg/l

Discussion

In this study, all the 24 carbapenem-resistant strains produced IMP-1 type MBL. Moreover, 16 of these strains contained the *intI-1* gene and 8 strains contained both the *intI-1* and *intI-3* integrons. These results suggested that *intI-1* was possibly linked with bla_{IMP-1}, but it remains to be discovered whether *intI-3* was closely linked with bla_{IMP-1}. These findings were in agreement with the report of Shibata et al.[7] The class 1 integron is the most common type detected among Gram-negative organisms in Japan. There were a few reports of Gram-negative bacteria which possess class 3 integrons, such as *Serratia marcescens* (Genbank accession no. AB070224) and *Klebsiella pneumoniae* (Genbank accession no. AY219651). Furthermore, the strains that possess

both class 1 and class 3 integrons have rarely been reported in clinical isolates of *P. putida*,[7] and their functional association is not clear.

The PFGE patterns of Pp7 and Pp17 strains suggested that these *P. putida* strains shared a common lineage. As for the other strains, since there was no great degree of similarity among them, there were unlikely to be a common source of infection.

The OprD protein allows the entry of carbapenems, and its reduced expression is frequently noted in carbapenem-resistant isolates of *P. aeruginosa* and *P. putida*.[5] We measured the expression of the *oprD* gene by semiquantitative RT–PCR. The expression was decreased in 21 carbapenem-resistant strains, which included 18 strains with relative *oprD* expression of 50%, or less than those of Pp1035. Although we did not confirm the role of OprD by inactivating the *oprD* gene via genetic means, these results suggested that the OprD expression might contribute to the carbapenem resistance.

Previous studies have demonstrated that multiple mutations in the QRDRs of DNA gyrase and topoisomerase IV are required for high-level fluoroquinolone resistance in *P. aeruginosa* and *P. putida*.[5,10] In this study, all isolates having CIP MICs of > 32 mg/l had a single substitution (Thr83Ile) in GyrA, and one strain (Pp12 having a CIP MIC of 512 mg/l) had double substitutions in GyrA (Thr83Ile) and ParC (Ser87Leu). As we describe the effects of the EPI later, CIP resistance was not fully affected by the EPI in the strain Pp12 (Table 3). It was thought that these double mutations mainly contributed to this resistance. This was the first time that a substitution of Ser87Leu in ParC has been detected in *P. putida*. In the present study, we did not find a clear relationship between the degree of CIP resistance and the number of substitutions in GyrA and ParC in *P. putida*. However, such a relationship might have been found if a larger number of isolates had been examined.

Several antibiotic efflux systems contributing to multidrug resistance (including resistance to carbapenems and fluoroquinolones) have been characterized in *P. aeruginosa*.[8,12] Although the existence of efflux pumps in *P. putida* has been confirmed,[14,15] their role in clinical isolates of *P. putida* remains unclear. In this regard, we found that IPM MICs decreased > 2-fold more with the EPI than without it in only 3 of the 24 carbapenem-resistant strains. Furthermore, we performed a similar experiment against MEM using PAβN or carbonyl cyanide *m*-chlorophenylhydrazone (CCCP, Sigma-Aldrich), but there was not a > 2-fold decrease of MICs with EPI (data not shown). This suggests that while overproduction of the efflux pump may in part contribute to the acquisition of resistance to carbapenems, production of MBL plays a major role in resistance to carbapenems in clinical isolates of *P. putida* in this study. Although a report has demonstrated that increasing efflux pump activity as a mechanism giving IPM resistance may be more important and/or occur frequently in *Acinetobacter baumannii*,[20] we could not clarify the reason why IPM MICs decreased with EPI in this study.

Efflux systems are also believed to be involved in reducing susceptibility to fluoroquinolones. Recently, DNA gyrase and topoisomerase IV mutations and efflux pumps were found to act synergistically in relation to the MICs of fluoroquinolones for *E. coli, Campylobacter* species, and *P. mirabilis*.[19,21,22] We found that all the 11 CIP-resistant strains were affected by it, and in 10 of these the presence of the EPI reduced MIC levels by more than 2-fold as compared with those in the absence of the EPI, although the level of the MICs with the EPI was still above the breakpoint of resistance. In this experiment, we increased the EPI concentration to 30 mg/l to see if the dose of the EPI affected the results, but this had very little effect (data not shown).

In contrast to the strain Pp12 described earlier, the strain Pp18, which had the same CIP MIC (512 mg/l) as the strain Pp12 but a single substitution (Thr83Ile) in GyrA, the CIP MIC was greatly reduced to 32 mg/l in the presence of the EPI. Therefore, it was thought that this resistance was mainly due to the efflux pump systems. These data indicate that mutations in DNA gyrase (and topoisomerase IV) and overproduction of efflux systems synergistically contributed to the acquisition of a high level of CIP resistance in our clinical isolates of *P. putida*.

Overall, our results showed that the production of IMP-1 MBL was largely responsible for developing a high level of resistance to carbapenems. In the case of CIP, our results indicate that mutation in DNA gyrase (and topoisomerase IV) and overproduction of the efflux pump synergistically contributed to a high level of resistance in the clinical isolates of *P. putida*.

Acknowledgment We thank Sankichi Horiuchi for valuable comments on this study. We did not receive any financial support from third parties.

References

1. Ladhani S, Bhutta ZA. Neonatal *Pseudomonas putida* infection presenting as staphylococcal scalded skin syndrome. Eur J Clin Microbiol Infect Dis 1998;17:642–4.
2. Fass RJ, Barnishan J, Solomon MC, Ayers LW. In vitro activities of quinolones, β-lactams, tobramycin, and trimethoprim–sulfamethoxazole against nonfermentative Gram-negative bacilli. Antimicrob Agents Chemother 1996;40:1412–8.
3. Lombardi G, Luzzaro F, Docquier JD, Riccio ML, Perilli M, Coli A, et al. Nosocomial infections caused by multidrug-resistant isolates of *Pseudomonas putida* producing VIM-1 metallo-β-lactamase. J Clin Microbiol 2002;40:4051–5.
4. Docquier JD, Riccio ML, Mugnaioli C, Luzzaro F, Endimiani A, Toniolo A, et al. IMP-12, a new plasmid-encoded metallo-β-lactamase from a *Pseudomonas putida* clinical isolate. Antimicrob Agents Chemother 2003;47:1522–8.
5. Horii T, Muramatsu H, Iinuma Y. Mechanisms of resistance to fluoroquinolones and carbapenems in *Pseudomonas putida*. J Antimicrob Chemother 2005;56:643–7.
6. Lee K, Lim JB, Yum JH, Yong DG, Chong YS, Kim JM, et al. blaVIM-2 cassette-containing novel integrons in metallo-β-lactamase-producing *Pseudomonas aeruginosa* and *Pseudomonas putida* isolates disseminated in a Korean hospital. Antimicrob Agents Chemother 2002;46:1053–8.
7. Shibata N, Yamane YDK, Yagi T, Kurokawa H, Shibayama K, Kato H, et al. PCR typing of genetic determinants for metallo-β-lactamases and integrases carried by Gram-negative bacteria isolated in Japan, with a focus on the class 3 integron. J Clin Microbiol 2003;41:5407–13.

8. Livermore DM. Of *Pseudomonas*, porins, pumps and carbapenems J Antimicrob Chemother 2001;47:247–50.
9. Kohler T, Michea-Hamzehpour M, Epp SF, Pechere JC. Carbapenem activities against *Pseudomonas aeruginosa*: respective contributions of OprD and efflux systems. Antimicrob Agents Chemother 1999;43:424–7.
10. Jalal S, Wretlind B. Mechanisms of quinolone resistance in clinical strains of *Pseudomonas aeruginosa*. Microb Drug Resist 1998;4: 257–61.
11. Hancock RE. Resistance mechanisms in *Pseudomonas aeruginosa* and other nonfermentative Gram-negative bacteria. Clin Infect Dis 1998;27 Suppl 1:S93–S99.
12. Li XZ, Nikaido H, Poole K. Role of MexA–MexB–OprM in antibiotic efflux in *Pseudomonas aeruginosa*. Antimicrob Agents Chemother 1995;39:1948–53.
13. Aeschlimann JR. The role of multidrug efflux pumps in the antibiotic resistance of *Pseudomonas aeruginosa* and other Gram-negative bacteria. Pharmacotherapy 2003;23:916–24.
14. Ramos JL, Duque E, Godoy P, Segura A. Efflux pumps involved in toluene tolerance in *Pseudomonas putida* DOT–T1E. J Bacteriol 1998;180:3323–9.
15. Kieboom J, de Bont JAM. Identification of molecular characterization of an efflux system involved in *Pseudomonas putida* S12 multidrug resistance. Microbiology 2001;147:43–51.
16. Fukumori F, Hirayama H, Takami H, Inoue A, Horikoshi K. Isolation and transposon mutagenesis of a *Pseudomonas putida* KT2442 toluene-resistant variant: involvement of an efflux system in solvent tolerance. Extremophiles 1998;2:395–400.
17. Clinical and Laboratory Standards Institute. Performance standards for antimicrobial susceptibility testing: 15th informational supplement M100-S15. Wayne: CLSI; 2005.
18. Renau TE, Leger R, Flamme EM, Sangalang J, She MW, Yen R, et al. Inhibitors of efflux pumps in *Pseudomonas aeruginosa* potentiate the activity of the fluoroquinolone antibacterial levofloxacin. J Med Chem 1999;42:4928–31.
19. Oethinger M, Kern WV, Jellen-Ritter AS, McMurry LM, Levy SB. Ineffectiveness of topoisomerase mutations in mediating clinically significant fluoroquinolone resistance in *Escherichia coli* in the absence of the AcrAB efflux pump. Antimicrob Agents Chemother 2000;44:10–3.
20. Wensi S. Hu, Shu-Man Yao, Chang-Phone Fung, Yi-Ping Hsieh, Chang-Pan Liu, Jing-Fang Lin. An OXA-66/OXA-51-like carbapenemase and possibly an efflux pump are associated with resistance to imipenem in *Acinetobacter baumannii*. Antimicrob Agents Chemother 2007;51:3844–52.
21. Ge BL, McDermott PF, White DG, Meng JH. Role of efflux pumps and topoisomerase mutations in fluoroquinolone resistance in *Campylobacter jejuni* and *Campylobacter coli*. Antimicrob Agents Chemother 2005;49:3347–54.
22. Saito R, Sato K, Kumita W, Inami N, Nishiyama H, Okamura N, et al. Role of type II topoisomerase mutations and AcrAB efflux pump in fluoroquinolone-resistant clinical isolates of *Proteus mirabilis*. J Antimicrob Chemother 2006;58:673–7.

Hepatology Research 2009; 39: 657–663 doi: 10.1111/j.1872-034X.2009.00517.x

Original Article

Chronic hepatitis C in patients co-infected with human immunodeficiency virus in Japan: a retrospective multicenter analysis

Hiroshi Yotsuyanagi,[1] Yoshimi Kikuchi,[2] Kunihisa Tsukada,[1,2] Kyouji Nishida,[3] Michio Kato,[4] Hironori Sakai,[5] Junki Takamatsu,[6] Shuhei Hige,[7] Kazuaki Chayama,[8] Kyoji Moriya[1] and Kazuhiko Koike[1]

[1]*Department of Internal Medicine, Graduate School of Medicine, University of Tokyo,* [2]*AIDS Clinical Center, International Medical Center of Japan,* [3]*Department of Laboratory Medicine, Tokyo Medical University, Tokyo,* [4]*Department of Gastroenterology, Osaka National Hospital, Osaka,* [5]*Department of Gastroenterology, Kyushu National Hospital, Fukuoka,* [6]*Division of Transfusion Medicine, Nagoya University Hospital, Nagoya,* [7]*Department of Gastroenterology and Hematology, Hokkaido University Graduate School of Medicine, Sapporo and* [8]*Department of Medicine and Molecular Science, Graduate School of Biomedical Sciences, Hiroshima University, Hiroshima, Japan*

Aim: A nationwide survey in Japan revealed that nearly one-fifth of human immunodeficiency virus (HIV)-positive patients are co-infected with hepatitis C virus (HCV). We conducted a study to further analyze the features of liver disease in HIV–HCV co-infected patients.

Methods: We analyzed 297 patients from eight hospitals belonging to the HIV/AIDS Network of Japan.

Results: HCV genotypes 1, 2, 3, 4 and mixed genotypes were detected in 55.2, 13.7, 18.9, 0.9 and 11.3% of patients, respectively, in contrast to the fact that only genotypes 1 and 2 are detected in HCV mono-infected patients in Japan. This is compatible with the transmission of HCV through imported blood products contaminated by HCV. Sixteen of 297 HIV–HCV co-infected patients had advanced liver disease accompanied by ascites, hepatic encephalopathy or hepatocellular carcinoma. The average age of such patients was 41.1 ± 14.0 years, which was much younger than that of HCV mono-infected patients with the same complications. The progression speed of liver disease estimated from the changes in the levels of serum albumin, bilirubin, or platelet was slower in patients who achieved sustained virological response with interferon treatment than in those who did not receive it. The overall sustained virological response rate to interferon treatment was 43.3%.

Conclusions: Our findings suggest that liver disease is more advanced in HIV–HCV co-infected patients than in HCV mono-infected patients, and interferon treatment may retard the progression of liver disease in such patients.

Key words: acquired immunodeficiency syndrome, chronic liver disease, genotype, interferon therapy

INTRODUCTION

THE PROGNOSIS OF human immunodeficiency virus (HIV) infection has markedly improved since the introduction of hyperactive anti-retroviral therapy (HAART).[1,2] Opportunistic infection has been prevented or properly managed, resulting in lower mortality rates. Liver disease, in particular related to hepatitis C virus (HCV) infection, has now become the main cause of mortality among HIV-infected patients on HAART in Western countries.[3,4] A national survey among Japanese HIV-infected patients with coagulation disorders has shown that the mortality rate related to HCV-related liver disease after 1997 was twofold that before 1997.[5] In Japan, therefore, HCV infection may also be a major cause of death in HIV–HCV co-infected patients. However, there has been no extensive analysis of liver disease in HIV–HCV co-infected patients in Japan.

Correspondence: Professor Kazuhiko Koike, Department of Infectious Diseases, Internal Medicine, Graduate School of Medicine, University of Tokyo, 7-3-1 Hongo, Bunkyo-ku, Tokyo 113-8655, Japan. Email: kkoike-tky@umin.ac.jp
Received 20 January 2009; revised 9 February 2009; accepted 10 February 2009.

Interferon (IFN) treatment in combination with ribavirin administration, which is now the first choice for HCV mono-infected patients,[6] is also a standard treatment for chronic hepatitis in HIV–HCV co-infected patients. Eradication of HCV is assumed to improve liver function, and normalization of serum aminotransferase (ALT) levels by IFN treatment may retard the progression of liver disease in HIV–HCV co-infected patients, even if they are on HAART. However, in general, the response rate to IFN treatment is lower in HIV–HCV co-infected patients than in HCV mono-infected patients.[7] The effects of IFN treatment on liver function and prognosis in HIV–HCV co-infected patients in Japan are yet undefined.

In 2004, we conducted a nationwide survey to determine the prevalence of HCV infection in HIV-infected patients by distributing a questionnaire to the hospitals in the HIV/AIDS Network of Japan, which revealed that 935 (19.2%) of 4877 HIV-positive patients were also positive for anti-HCV antibody.[8] In this study, we analyzed the progression of liver diseases and the impact of IFN treatment on the parameters of liver function in HIV–HCV co-infected patients in a multicenter retrospective study.

METHODS

Registry of patients with HIV–HCV co-infection

THE QUESTIONNAIRE REGARDING the current state of HIV–HCV co-infection was sent to the 366 hospitals in the HIV/AIDS Network of Japan in 2004, sponsored by the Japanese Ministry of Health, Labour and Welfare. One hundred seventy-six hospitals (48.1%) responded. The results, already published,[8] showed that HIV–HCV co-infected patients are concentrated in particular hospitals in big cities around Japan. Among these hospitals, we chose three hospitals in the Tokyo metropolitan area, and one each in the Hokkaido, Chubu, Osaka, Chugoku and Kyushu areas. These eight hospitals belong to the HIV/AIDS Network and had more HIV–HCV co-infected patients than other hospitals.

In the study, the following information was obtained from the hospitals regarding each HIV–HCV co-infected patient who visited the hospitals at least once between January and December in 2004: (1) age and sex of HIV-positive patients with anti-HCV; (2) possible transmission routes of HIV; (3) history of habitual alcohol intake; (4) date of the first and last visits; (5) counts of white blood cells, CD4-positive lymphocytes and platelets at the first and last visits; (6) levels of serum albumin and bilirubin at the first and last visits; (7) levels of HIV-RNA and HCV-RNA at the first and last visits; (8) history of IFN treatment with or without ribavirin; (9) history of HAART; and (10) history of jaundice, ascites, hepatic encephalopathy and hepatocellular carcinoma (HCC). The study sheets were completed by the physicians in charge and sent to the Department of Internal Medicine, University of Tokyo.

Ethical issues

The protocol of the current survey was approved by the ethical committee of each institution, and written informed consent was obtained from each patient.

Statistical analysis

The collected data were analyzed using Mann–Whitney's *U*-test whenever appropriate. *P*-values less than 0.05 were regarded as statistically significant.

RESULTS

Clinical backgrounds of registered patients

FROM THE EIGHT hospitals, 297 patients were registered. The number, age, sex, estimated transmission routes and history of habitual alcohol intake are shown in Table 1. Two hundred and ninety (97.6%) were male patients. The mean age of the patients was 37.9 ± 10.3.

HCV genotype was determined in 212 patients. One hundred seventeen (55.2%) patients were infected by genotype 1 HCV. Infection by genotypes 2, 3 or 4 HCV was found in 29 (13.7%), 40 (18.9%) and 2 (0.9%) patients, respectively. Twenty-four (11.3%) patients were infected by HCV of mixed genotypes. In the remaining 85 patients, the genotype was indeterminable or undetermined. The mean ages of patients infected by different HCV genotypes were similar (Table 1).

In 259 (87.2%) of 297 registered patients, HIV was most probably transmitted through the administration of blood products. Other transmission routes were sexual contacts among men who have sex with men (MSM) (4.0%), heterosexual contacts (3.0%) and intravenous drug use (IDU) (0.3%). Habitual alcohol consumption was noted in only one patient with genotype 1 HCV (0.6%).

Outcomes of IFN treatment in HIV–HCV co-infected patients

Serum HCV-RNA levels were available both at the first visit and registry to the study (i.e. the end of observa-

Table 1 Demography, transmission route and HCV genotypes in HIV–HCV co-infected patients

HCV genotype	Number (%)	HCV sub-genotypes	Viral load† (High : Low)	Age	Sex (Male : Female)	Transmission route				
						Transfusion	MSM	Hetero-sexual	IDU	Others
1	117 (55.2)	1a 31, 1b 43, 1a+1b 31, undetermined 12	31:11	38.3 ± 10.4	114:3	102	7	1	0	7
2	29 (13.7)	2a 16, 2b 11, undetermined 2	5:5	39.8 ± 9.5	29:0	24	1	1	0	3
3	40 (18.9)	3a 40	12:2	36.1 ± 8.9	40:0	38	0	0	0	2
4	2 (0.9)	4a 2	2:0	38.5 ± 2.1	2:0	2	0	0	0	0
Mixed	24 (11.3)	2a+3a 6, 1b+3a 3, others 15	11:0	38.7 ± 8.7	24:0	24	0	0	0	0
Others	85	Undetermined 85	6:1	36.2 ± 11.5	81:4	69	4	7	1	4
Total	297		67:19	37.9 ± 10.3	290:7	259 (87.2%)	12 (4.0%)	9 (3.0%)	1 (0.3%)	16 (5.5%)

†Viral loads are available in only a subset of patients. High viral load: more than 1 Meq/mL by branched DNA-probe assay or more than 100 KIU/mL by Amplicor monitor assay.
HCV, hepatitis C virus; HIV, human immunodeficiency virus; IDU, intravenous drug users; MSM, men who have sex with men.

tion) in 158 patients. Of these 158, 60 patients (38.0%) received IFN treatment for HCV, and 35 of these 60 patients did it in combination with ribavirin. Those who did not complete the scheduled treatment were excluded from the current analysis.

As shown in Table 2, 26 (43.3%), 11 (18.4%) and 23 (38.3%) of the treated patients achieved sustained virological response (SVR), end-of-treatment virological response (ETR) and no virological response (NR), respectively. The SVR rate in patients with each genotype is shown in Table 2. The SVR rate in the patients who underwent IFN treatment in combination with ribavirin was 31.4% in total. The SVR rate in patients with each genotype who underwent IFN/ribavirin combination therapy is shown in Table 2.

All of the 26 patients who achieved SVR remained negative for serum HCV-RNA in the further follow-up periods. In contrast, none of the patients with ETR or NR became negative for serum HCV-RNA in the follow-up periods. In five patients who did not receive IFN treatment, HCV-RNA was negative at the end of the observation period, although it was positive at least twice before the registry. The profiles of the five patients are shown in Table 3.

Changes in liver function and associated complications (Table 4)

As mentioned above, the data on liver function and serum HCV-RNA positivity were available both at the first visit and registry (end of observation) in 158 of the 297 registered patients. The mean observation period was 9.5 ± 5.0 and 8.2 ± 8.2 years in the IFN-treated and IFN-untreated patients, respectively. Unfortunately, few, if any, patients underwent liver biopsy, because most HIV–HCV co-infected patients had coagulation disorders.

The annual change in the serum albumin concentration was +0.05 ± 0.42 g/dL in the IFN-treated patients, and −0.80 ± 0.82 g/dL in the non-IFN-treated patients. The annual change in the serum bilirubin concentration was +0.08 ± 0.38 mg/dL in the IFN-treated patients, while it was +0.15 ± 0.15 mg/dL in the non-IFN-treated patients. Among the IFN-treated patients, the serum bilirubin concentration decreased by 0.02 ± 0.08 mg/dL in the patients who achieved SVR, which was significantly larger than that in the non-IFN-treated patients at the end of the observation ($P < 0.05$). The annual changes in platelet counts were +0.06 ± 1.13 ($\times 10^4/\mu l$) in the IFN-treated patients and −0.94 ± 0.95 ($\times 10^4/\mu l$) in the non-IFN-treated patients. The change in platelet

Table 2 Virological response to interferon treatment in HIV–HCV co-infected patients

Genotype	Viral load (High : Low)†	Response			Total
		SVR	ETR	NR	
(a) Response to interferon treatment in total (with or without ribavirin)					
1	9:6	7 (33.3%)	1	13	21
2	5:3	4 (40.0%)	2	4	10
3	5:1	5 (62.5%)	1	2	8
4	1:0	0	1	0	1
Mixed	5:1	2 (33.3%)	3	1	6
Others	6:2	8 (57.1%)	3	3	14
Total	31:13	26 (43.4%)	11	23	60
(b) Response to ribavirin/interferon combination therapy including peginterferon					
1	8:2	2 (15.3%)	0	11	13
2	1:2	1 (25.0%)	0	3	4
3	4:1	4 (66.7%)	1	1	6
4	1:0	0	1	0	1
Mixed	4:1	1 (20.0%)	3	1	5
Others	3:0	3 (50.0%)	1	2	6
Total	21:6	11 (31.4%)	6	18	35

†Viral loads are available in only a subset of patients. High viral load: more than 1 Meq/mL by Branched DNA-probe assay or more than 100 KIU/mL by Amplicor monitor assay.
ETR, end of treatment virological response; NR, no virological response; SVR, sustained virological response.

counts in the patients who achieved SVR was significantly larger than that in the non-IFN-treated patients ($P < 0.05$, Table 4).

No symptoms of hepatic failure (ascites or hepatic encephalopathy) were observed in the 60 IFN-treated patients while they were observed in six of the 98 non-IFN-treated patients. HCC was found in one IFN-treated patient after SVR, while it was found in two non-IFN-treated patients (Table 4).

Impact of HAART on liver function and associated complications (Table 5)

Information on HAART was available in 292 patients. The mean observation periods were 8.4 ± 4.2 years in 234 patients on HAART, and 9.8 ± 6.0 years in 58 patients not on HAART. Changes in the levels of albumin, bilirubin or platelet were similar between the two groups (statistically not significant). The morbidities of hepatic decompensation symptoms (ascites and hepatic encephalopathy) and HCC were not significantly different between the two groups. In total, nine patients had hepatic decompensation and seven had HCC, and the average age of such patients was 41.1 ± 14.0 years, which was much younger than that of HCV mono-infected patients with the same complications.[9]

DISCUSSION

IN THE CURRENT study, the features of liver disease in HIV–HCV co-infected patients in Japan were analyzed. The determination of HCV genotypes revealed that genotype 3 or 4, which is rarely seen in HCV mono-infected patients in Japan,[10] was found in a substantial fraction of HIV-infected patients. In addition, some of these patients were infected with HCV of mixed genotypes. These results are compatible with the fact that HCV is transmitted through imported blood products that were contaminated by HCV, as is the case with HIV infection.[11] Infection by HCV of mixed genotypes may reflect frequent administrations of blood products of different lots.

We evaluated the response rate to IFN treatment in HIV–HCV co-infected patients in Japan. Because the IFN treatment protocol varied between facilities, it was not easy to evaluate the effects of the treatments including IFN in this cohort. However, the regimen of ribavirin/IFN combination therapy was similar between the hospitals: the treatment period was 24 weeks in patients with HCV genotypes 2 and 3, and 48 weeks in those with HCV of other genotypes when either pegylated or standard IFN in combination with ribavirin was used.[12] Therefore, it may be possible to estimate the effect

Table 3 Clinical backgrounds of patients who spontaneously cleared HCV in HIV-infected patients

Patient no.	Age	Sex	Transmission route	Observation period (years)	HCV-RNA (KIU/mL)	HCV genotype	HIV-RNA ($\times10^2$/mL)	WBC (/μL)	CD4+ T cells (/μL)	Platelets ($\times10^4$/mL)	ALT (U/l)	HAART
1	33	M	Transfusion	8.8	290	ND	200 000	4500	5	26.3	21	Yes
2	31	M	MSM	2.3	Positive†	ND	13 000	5760	931	22.7	29	Yes
3	27	M	Transfusion	9.3	>850	3a	180 000	4000	51	10.1	84	Yes
4	53	M	Transfusion	4.5	Positive†	1a	20 000	4800	296	35.4	24	No
5	22	M	Transfusion	7.8	220	ND	990	5500	125	33.1	44	Yes

†Positive: HCV-RNA was positive by qualitative PCR, but was not quantitatively determined.
ALT, aminotransferase; HAART, highly active anti-retroviral therapy; HCV, hepatitis C virus; HIV, human immunodeficiency virus; MSM, men who have sex with men; ND, not determined; WBC, white blood cells.

Table 4 Changes in clinical parameters and IFN treatment in HIV–HCV co-infected patients

	Outcome of IFN treatment	Number	Observation period (years)	⊿Albumin†	⊿Bilirubin‡	⊿Platelet§	Ascites/ encephalopathy	HCC
IFN-treated patients		60	9.5 ± 5.0	0.05 ± 0.42	0.08 ± 0.38*	0.06 ± 1.13	0	1
	SVR	26	9.1 ± 4.4	0.13 ± 0.59	(−) 0.02 ± 0.08*	0.14 ± 0.76*	0	1
	ETR	11	14.6 ± 7.0	(−) 0.07 ± 0.14	0.51 ± 1.04	0.07 ± 1.50	0	0
	NR	23	7.4 ± 2.0	0.01 ± 0.30	0.09 ± 0.30	(−) 0.18 ± 0.32	0	0
Non-IFN-treated patients		98	8.2 ± 8.2	(−) 0.80 ± 0.82	0.15 ± 0.15	(−) 0.94 ± 0.95	6	2
All		158	8.7 ± 4.7	(−) 0.45 ± 2.93	0.13 ± 0.52	(−) 0.59 ± 3.78	6	3

*$P < 0.05$ versus patients without IFN treatment.
†⊿Albumin: changes in albumin concentration (g/dL)/observation period (years).
‡⊿Bilirubin: changes in bilirubin concentration (mg/dL)/observation period (years).
§⊿Platelet: changes in platelet count ($\times10^4$/μL)/observation period (years).
ETR, end of treatment virological response; HCC, hepatocellular carcinoma; HCV, hepatitis C virus; HIV, human immunodeficiency virus; IFN, interferon; NR, no virological response; SVR, sustained virological response.

Table 5 Changes in clinical parameters and HAART in HIV–HCV co-infected patients

	Number	Age	Sex (M : F)	Observation period (years)	⊿Albumin†	⊿Bilirubin‡	⊿Platelet§	IFN	Ascites/ encephalopathy	HCC
HAART (+)	234	37.8 ± 10.4	227:7	8.4 ± 4.2	(−) 0.002 ± 0.18	0.13 ± 0.53	(−) 0.40 ± 3.71	143 (61.1%)	6	5
HAART (−)	58	38.1 ± 10.5	58:0	9.8 ± 6.0	(−) 0.14 ± 0.18	0.03 ± 0.25	(−) 1.40 ± 3.30	30 (51.7%)	3	2

†⊿Albumin: changes in albumin concentration (g/dL)/observation period (years).
‡⊿Bilirubin: changes in bilirubin concentration (mg/dL)/observation period (years).
§⊿Platelet: changes in platelet count ($\times 10^4$/[L])/observation period (years).
HAART, highly active anti-retroviral therapy; HCC, hepatocellular carcinoma; HCV, hepatitis C virus; HIV, human immunodeficiency virus.

of ribavirin/IFN combination therapy in HIV–HCV co-infected patients in this study.

The response rate to ribavirin/IFN combination therapy was 31.4% in total, and 15.3% in patients with HCV genotype 1, which are comparable rates to those achieved in previous studies on HIV–HCV co-infected patients in Western countries.[7] The low response rate in HIV–HCV co-infected patients compared with HCV mono-infected patients[12] may be attributed to several factors: impaired immune response, high HCV loads and viral quasi-species caused by frequent chances of transmission. Of these, high viral loads may be essential, because Table 2 shows that patients with genotype 1 HCV achieved SVR even by IFN monotherapy if their viral loads were low. In the era of IFN monotherapy, patients with favorable conditions were treated first of all: pretreatment viral loads in patients who received IFN monotherapy were lower than those who received PEG-IFN–ribavirin combination therapy. This may be the reason why the efficacy of PEG-IFN–ribavirin combination therapy was lower than that with IFN monotherapy in this study.

The serum bilirubin concentrations and platelet counts were improved in the patients who achieved SVR by IFN treatment. Although the response rate to IFN treatment is lower in HIV–HCV co-infected patients than in HCV mono-infected patients, the overall benefit of IFN treatment on liver function may be similarly expected in the patients who achieved SVR. HAART showed no impact on the liver function in HIV–HCV co-infected patients. Improvement of liver function can be expected only in IFN-treated patients, although there is a possibility that only patients with preserved liver function were able to receive IFN treatment. Given that liver disease is the major life-threatening factor in HIV-infected patients, IFN treatment should be considered in the early stage of HIV–HCV co-infection.

It should be noted that nine patients had hepatic decompensation and seven had HCC, and the average age of such patients was much younger than that of HCV mono-infected patients with the same complications.[9] This finding is compatible with reports from Western countries showing a faster progression of fibrosis[13] and earlier development of HCC.[14] A possibly interesting finding is that five patients (approximately 3% of patients whose serum HCV-RNA level was serially determined) cleared HCV-RNA from the serum without IFN treatment. Previous reports showed that some HIV-infected patients could spontaneously clear HCV-RNA.[15–17] The clearance of HCV among patients with chronic HCV infection is rare, although it has been

reported in Japan.[18] Three of the five patients had high HCV loads and low $CD4^+$ T-lymphocyte counts, which are generally thought to be unfavorable for spontaneous HCV clearance. A difference in immune status of HIV-infected patients from HCV mono-infected patients may be involved in such an observation, although further studies are awaited.

In summary, our study demonstrated that approximately 20% of HIV-infected patients are co-infected with HCV. Some of the HIV–HCV co-infected patients had advanced liver disease such as ascites, encephalopathy or HCC at a younger age than HCV mono-infected patients, suggesting that the progression of liver disease may be more rapid in HIV–HCV co-infected patients than in HCV-mono-infected ones. Treatments with regimens including IFN, which may improve liver function and decrease liver-related death, should be considered in HIV–HCV co-infected patients.

ACKNOWLEDGMENTS

WE THANK MS Ogawa for her assistance in the questionnaire inquiry. This work was supported in part by Health Sciences Research Grants from the Ministry of Health, Labour and Welfare of Japan (AIDS Research).

REFERENCES

1 Simon V, Ho DD, Karim QA. HIV/AIDS epidemiology, pathogenesis, prevention, and treatment. *Lancet* 2006; **368**: 489–504.
2 Schneider MF, Gange SJ, Williams CM *et al.* Patterns of the hazard of death after AIDS through the evolution of antiretroviral therapy: 1984–2004. *AIDS* 2005; **19**: 2009–18.
3 Kramer JR, Giordano TP, Souchek J, El-Serag HB Hepatitis C coinfection increases the risk of fulminant hepatic failure in patients with HIV in the HAART era. *J Hepatol* 2005; **42**: 309–14.
4 Merchante N, Giron-Gonzalez JA, Gonzalez-Serrano M *et al.* Survival and prognostic factors of HIV-infected patients with HCV-related end-stage liver disease. *AIDS* 2006; **20**: 49–57.
5 Tatsunami S, Taki M, Shirahata A, Mimaya J, Yamada K. Increasing incidence of critical liver disease among causes of death in Japanese hemophiliacs with HIV-1. *Acta Haematol* 2004; **111**: 181–4.
6 Shiffman ML. Optimizing the current therapy for chronic hepatitis C virus: peginterferon and ribavirin dosing and the utility of growth factors. *Clin Liver Dis* 2008; **12**: 487–505.
7 Lo Re V 3rd, Kostman JR, Amorosa VK. Management complexities of HIV/hepatitis C virus coinfection in the twenty-first century. *Clin Liver Dis* 2008; **12**: 587–609.
8 Koike K, Tsukada K, Yotsuyanagi H *et al.* Prevalence of coinfection with human immunodeficiency virus and hepatitis C virus in Japan. *Hepatol Res* 2007; **37**: 2–5.
9 Okita K. Clinical aspects of hepatocellular carcinoma in Japan. *Intern Med* 2006; **45**: 229–33.
10 Hayashi N, Takehara T. Antiviral therapy for chronic hepatitis C: past, present, and future. *J Gastroenterol* 2006; **41**: 17–27.
11 Yamaguchi T, Hashimoto S, Oka S *et al.* Physical condition and activity of daily living among HIV patients infected through blood products in Japan. *J Epidemiol* 2002; **12**: 383–93.
12 Okanoue T, Itoh Y, Minami M *et al.* Guidelines for the antiviral therapy of hepatitis C virus carriers with normal serum aminotransferase based on platelet counts. *Hepatol Res* 2008; **38**: 27–36.
13 Benhamou Y, Bochet M, Di Martino V *et al.* Liver fibrosis progression in human immunodeficiency virus and hepatitis C virus coinfected patients. The Multivirc Group. *Hepatology* 1999; **30**: 1054–8.
14 Bräu N, Fox RK, Xiao P *et al.* Presentation and outcome of hepatocellular carcinoma in HIV-infected patients: a U.S.–Canadian multicenter study. *J Hepatol* 2007; **47**: 527–37.
15 Shores NJ, Maida I, Soriano V, Nunez M. Sexual transmission is associated with spontaneous HCV clearance in HIV-infected patients. *J Hepatol* 2008; **49**: 323–8.
16 Falconer K, Gonzalez VD, Reichard O, Sandberg JK, Alaeus A Spontaneous HCV clearance in HCV/HIV-1 coinfection associated with normalized CD4 counts, low level of chronic immune activation and high level of T cell function. *J Clin Virol* 2008; **41**: 160–3.
17 Soriano V, Mocroft A, Rockstroh J *et al.* Spontaneous Viral Clearance, Viral Load, and Genotype Distribution of Hepatitis C Virus (HCV) in HIV-Infected Patients with Anti-HCV Antibodies in Europe. *J Infect Dis* 2008; **198**: 1337–44.
18 Sugiyasu Y, Yuki N, Nagaoka T *et al.* Histological improvement of chronic liver disease after spontaneous serum hepatitis C virus clearance. *J Med Virol* 2003; **69**: 41–9.

International Journal of Antimicrobial Agents 34 (2009) 347–350

Contents lists available at ScienceDirect

International Journal of Antimicrobial Agents

journal homepage: http://www.elsevier.com/locate/ijantimicag

Short communication

Analysis of plasmid-mediated multidrug resistance in *Escherichia coli* and *Klebsiella oxytoca* isolates from clinical specimens in Japan

Takashi Ode[a,*], Ryoichi Saito[b], Wakako Kumita[a], Kenya Sato[a], Shu Okugawa[b], Kyoji Moriya[b], Kazuhiko Koike[b], Noboru Okamura[a]

[a] *Department of Microbiology and Immunology, Graduate School of Health Sciences, Tokyo Medical and Dental University, 1-5-45 Yushima, Bunkyo-ku, Tokyo 113-8510, Japan*
[b] *Department of Infection Control and Prevention, The University of Tokyo Hospital, 7-3-1 Hongo, Bunkyo-ku, Tokyo 113-8655, Japan*

ARTICLE INFO

Article history:
Received 19 March 2009
Accepted 18 May 2009

Keywords:
qnr
Aminoglycoside acetyltransferase
Extended-spectrum β-lactamase
Metallo-β-lactamase
Class 1 integron

ABSTRACT

This study investigated the relationship of plasmid-mediated quinolone resistance (PMQR) and aminoglycoside resistance among oxyimino-cephalosporin-resistant *Escherichia coli* ($n = 46$) and *Klebsiella oxytoca* ($n = 28$) clinical isolates in Japan. Seventy-three isolates appeared to produce an extended-spectrum β-lactamase (ESBL) and one *K. oxytoca* isolate produced IMP-1 metallo-β-lactamase (MBL). Polymerase chain reaction (PCR) and sequencing confirmed that eight CTX-M-9/SHV-12-producing isolates, one IMP-1-producing *K. oxytoca* isolate, and six ESBL-positive *E. coli* isolates respectively possessed PMQR genes *qnrA1*, *qnrB6*, and *aac(6′)-Ib-cr*. All *qnr*-positive isolates also carried either *aac(6′)-Ib* or *aac(6′)-IIc* aminoglycoside acetyltransferase genes. Resistance determinants to β-lactams, quinolones and aminoglycosides were co-transferred with a plasmid of ca. 140 kb. The *qnrA1* gene was located downstream of insertion sequence *ISCR1* in complex class 1 integrons. A novel *qnrA1*-carrying class 1 integron with the cassette arrangement *aac(6′)-IIc–aadA2* as well as a unique class 1 integron with bla_{IMP-1}*–aac(6′)-IIc* cassettes on the plasmid carrying *qnrB6* were found in *K. oxytoca* isolates. We describe the identification of *qnrB6* and *aac(6′)-Ib-cr* and the close association of *qnr* with *aac(6′)-Ib* and *aac(6′)-IIc* for the first time in clinical isolates producing ESBL or MBL in Japan.

1. Introduction

Quinolone resistance is usually caused by chromosomal mutations, however the plasmid-mediated quinolone resistance (PMQR) determinants QnrA, QnrB, QnrS and AAC(6′)-Ib-cr have been described [1]. Although these PMQR determinants result in low-level quinolone resistance, such reduced susceptibility is important because it facilitates the selection of mutants with higher-level resistance. In Japan, although *qnrS* was first found in *Shigella flexneri* [2] and *qnrA* was also described in Enterobacteriaceae clinical isolates [3,4], the presence of clinical strains harbouring *qnrB* or *aac(6′)-Ib-cr* has not been reported. Furthermore, a recent prevalence study of *qnr* and the *qepA* plasmid-mediated efflux pump gene suggested a low prevalence of *Escherichia coli* harbouring *qepA* or *qnr* in Japan [5].

Many studies have shown that most *qnrA*-positive enterobacterial isolates are associated with plasmid-mediated AmpC-type β-lactamases, extended-spectrum β-lactamases (ESBLs) and metallo-β-lactamases (MBLs) [1,3,4,6,7]. *qnrA* is often located in complex class 1 integrons between common region 1 (CR1), comprising orf513 recombinase and a second copy of the 3′ conserved segment (3′-CS2), together with other resistance gene cassettes such as trimethoprim and aminoglycoside resistance cassettes [1]. However, little has been reported on the genetic context of *qnr* in Japan.

The present study was conducted to investigate the genetic relationship of the PMQR genes *qnr* and *aac(6′)-Ib-cr* as well as the 6′-*N*-aminoglycoside acetyltransferase [AAC(6′)] genes *aac(6′)-Ib* and *aac(6′)-IIc* among oxyimino-cephalosporin-resistant *E. coli* and *Klebsiella oxytoca* clinical isolates in Japan and to determine the structure of class 1 integrons, including the insertion sequence CR1 (*ISCR1*) element associated with *qnr*.

2. Materials and methods

2.1. Bacterial strains

A total of 46 *E. coli* and 28 *K. oxytoca* clinical isolates resistant to one or more of cefotaxime, ceftazidime and aztreonam, collected at the University of Tokyo Hospital (Tokyo, Japan) between November 2005 and October 2006, were examined in this study.

* Corresponding author. Tel.: +81 3 5803 4515; fax: +81 3 5803 5375.
E-mail addresses: takashi.ode.mt@gmail.com, takashi.0630@jcom.home.ne.jp (T. Ode).

0924-8579/$ – see front matter © 2009 Elsevier B.V. and the International Society of Chemotherapy. All rights reserved.
doi:10.1016/j.ijantimicag.2009.05.007

2.2. Susceptibility testing

ESBL and MBL production was confirmed by double-disk synergy tests using clavulanic acid and ethylene diamine tetra-acetic acid (EDTA) as β-lactamase inhibitors, respectively. Minimum inhibitory concentrations (MICs) of amikacin, aztreonam, cefazolin, cefoperazone, cefotaxime, ceftazidime, ciprofloxacin, gentamicin, imipenem, levofloxacin and meropenem were determined by the broth microdilution method according to the Clinical and Laboratory Standards Institute [8]. Etest (AB BIODISK, Solna, Sweden) was used to detect low-level reduction in ciprofloxacin and levofloxacin susceptibility. Quality control for the MICs was performed using the reference strains *Staphylococcus aureus* ATCC 21293, *E. coli* ATCC 25922 and *Pseudomonas aeruginosa* ATCC 27853.

2.3. Polymerase chain reaction (PCR) and sequencing

PCR amplification was performed with Premix *Taq* enzyme (Takara Bio, Shiga, Japan) according to the manufacturer's instructions. Both strands of the purified PCR fragments were sequenced with an ABI PRISM 3130 DNA sequencer (Applied Biosystems, Foster City, CA) and a similarity search was conducted using the BLAST program (DDBJ, Shizuoka, Japan).

2.4. Characterisation of β-lactamases

The bla_{TEM}, bla_{SHV} and bla_{CTX-M} genes were amplified using the published primers [9,10]. The presence of MBL genes bla_{IMP} and bla_{VIM} was tested with type-specific primers described previously [11]. For all *qnr*-positive isolates, the nucleotide sequences of the *bla* genes were determined by sequencing.

2.5. Detection of the plasmid-mediated quinolone resistance determinants and the AAC(6′) genes

Screening for *qnrA*, *qnrB* and *qnrS* was carried out by multiplex PCR amplification as described previously [12]. Sequences of *qnrA* and *qnrB* were determined by PCR sequencing with primers 5′-TTGATAAAGTTTTTCAGCAA and 5′-CTAATCCGGCAGCACTATTA for *qnrA1* and primers 5′-ATGACGCCATTACTGTAT and 5′-CTAACCAATCACCGCGAT for *qnrB6*, designed to amplify a 647-bp fragment and a 681-bp fragment, respectively. The presence of *aac(6′)-Ib* and *aac(6′)-Ib-cr* variant was determined by PCR sequencing using a common primer pair [13]. The primer pair used for detection of *aac(6′)-IIc* was 5′-CCAACAATGCCGCAATAGTT and 5′-ATGACCACTTCCCCTTGATT, amplifying a 573-bp fragment, designed in the present study.

2.6. Conjugation experiments and extraction of plasmids

Conjugation experiments were performed in Luria–Bertani broth with nine *qnr*-positive clinical isolates as donors and an *E. coli* C600 strain as recipient. Transconjugant clones were selected on Drigalski agar (BTB agar) plates containing 100 mg/L rifampicin and 4 mg/L cefotaxime (or 0.03 mg/L ciprofloxacin in the absence of transfer with cefotaxime). Plasmid DNA was extracted from donors and transconjugants using a NucleoBond® Xtra Midi (Macherey-Nagel, Düren, Germany) according to the manufacturer's instructions and was subjected to electrophoresis on 0.7% (w/v) agarose (Takara Bio) gel with ethidium bromide at 50 V for 3 h. The size of transferred plasmids was estimated by adding up EcoRI and NotI restriction fragments.

2.7. Analysis of the genetic environment of qnr and class 1 integron structures

The genetic context of the *qnr* genes was investigated by PCR mapping and subsequent sequencing as described previously [14]. The content and order of the gene cassettes inserted between the 5′ conserved segment (5′-CS) and 3′-CS1 were determined by sequencing as described previously [15]. Finally, the regions between *intI1* in 5′-CS and a second copy of *qacEΔ1* in 3′-CS2 were sequenced using a primer walking strategy.

Table 1
Antibiotic resistance genes and susceptibility profiles in donors (*qnr*-positive isolates), the *Escherichia coli* recipient and transconjugants.

Strain	Genotype of			Cassette array[a]	MIC (mg/L)										
	Qnr	β-Lactamase	AAC(6′)		CIP	LVX	CFZ	CFP	CTX	CAZ	ATM	IPM	MEM	GEN	AMK
Escherichia coli (donors)															
E5	*qnrA1*	bla_{TEM-1}, $bla_{CTX-M-9}$	*aac(6′)-Ib*	[*aadB–aadA2*]	>64	32	>128	>128	16	<1	2	≤1	≤1	>128	32
E15	*qnrA1*	bla_{SHV-12}	*aac(6′)-Ib*	[*dfr16–aadA2*]	≤0.5	≤0.5	>128	32	32	>64	>64	≤1	≤1	≤2	8
E18	*qnrA1*	bla_{SHV-12}	*aac(6′)-Ib*	[*dfr16–aadA2*]	≤0.5	≤0.5	>128	16	8	>64	>64	≤1	≤1	≤2	8
Klebsiella oxytoca (donors)															
K5	*qnrA1*	bla_{TEM-1}, $bla_{CTX-M-9}$	*aac(6′)-IIc*	[*aadB–aadA2*]	≤0.5	≤0.5	>128	64	8	≤1	4	≤1	≤1	8	≤2
K7	*qnrA1*	$bla_{CTX-M-9}$	*aac(6′)-Ib*	[*aadB–aadA2*]	≤0.5	≤0.5	>128	>128	8	2	>64	≤1	≤1	8	8
K9	*qnrA1*	bla_{TEM-1}, $bla_{CTX-M-9}$	*aac(6′)-IIc*[b]	[*aac(6′)-IIc–aadA2*]	≤0.5	2	>128	64	8	2	8	≤1	≤1	8	≤2
K10	*qnrA1*	bla_{TEM-1}, $bla_{CTX-M-9}$	*aac(6′)-IIc*	[*aadB–aadA2*]	≤0.5	2	>128	64	8	≤1	4	≤1	≤1	4	≤2
K16	*qnrA1*	bla_{TEM-1}, $bla_{CTX-M-9}$	*aac(6′)-IIc*	[*aadB–aadA2*]	≤0.5	2	>128	64	4	≤1	4	≤1	≤1	8	≤2
K27	*qnrB6*	bla_{IMP-1}[b]	*aac(6′)-IIc*[b]	[bla_{IMP-1}–*aac(6′)-IIc*]	1	2	>128	>128	32	>64	≤1	2	4	≤1	≤2
E. coli C600 (recipient)					0.016	0.032	≤2	≤8	≤1	≤1	≤1	≤1	≤1	≤1	≤2
Transconjugants[c]															
E5TC-cip	*qnrA1*	bla_{TEM-1}, $bla_{CTX-M-9}$	*aac(6′)-Ib*	[*aadB–aadA2*]	0.25	0.25	N.T.	N.T.	8	≤1	≤1	≤1	≤1	64	32
E15TC-cip	*qnrA1*	bla_{SHV-12}	*aac(6′)-Ib*	[*dfr16–aadA2*]	0.25	0.25	N.T.	N.T.	32	32	64	≤1	≤1	≤1	16
E18TC-cip	*qnrA1*	bla_{SHV-12}	*aac(6′)-Ib*	[*dfr16–aadA2*]	0.125	0.125	N.T.	N.T.	8	16	>64	≤1	≤1	≤1	8
K5TC-ctx	N.D.	bla_{TEM-1}, $bla_{CTX-M-9}$	*aac(6′)-IIc*	N.D.	0.016	0.016	>32	>32	16	≤1	>16	≤1	≤1	8	≤2
K9TC-ctx	*qnrA1*	bla_{TEM-1}, $bla_{CTX-M-9}$	*aac(6′)-IIc*[b]	[*aac(6′)-IIc–aadA2*]	0.25	0.25	>32	>32	32	≤1	>16	≤1	≤1	>8	≤2
K10TC-ctx	*qnrA1*	bla_{TEM-1}, $bla_{CTX-M-9}$	*aac(6′)-IIc*	[*aadB–aadA2*]	0.25	0.125	>32	>32	16	≤1	8	≤1	≤1	4	≤2
K16TC-ctx	N.D.	bla_{TEM-1}, $bla_{CTX-M-9}$	N.D.	N.D.	0.016	0.016	>32	>32	16	≤1	>16	≤1	≤1	≤1	≤2
K16TC-cip	*qnrA1*	bla_{TEM-1}, $bla_{CTX-M-9}$	*aac(6′)-IIc*	[*aadB–aadA2*]	0.25	0.25	N.T.	N.T.	32	≤1	4	≤1	≤1	8	4
K27TC-ctx	*qnrB6*	bla_{IMP-1}[b]	*aac(6′)-IIc*[b]	[bla_{IMP-1}–*aac(6′)-IIc*]	0.125	0.25	N.T.	N.T.	>16	>64	≤1	2	4	≤1	2

MIC, minimum inhibitory concentration; CIP, ciprofloxacin; LVX, levofloxacin; CFZ, cefazolin; CFP, cefoperazone; CTX, cefotaxime; CAZ, ceftazidime; ATM, aztreonam; IPM, imipenem; MEM, meropenem; GEN, gentamicin; AMK, amikacin; N.T., not tested; N.D., not detected.

[a] Gene cassette array in class 1 integrons.

[b] Genes carried as cassettes by the class 1 integrons.

[c] cip, transconjugants selected by ciprofloxacin; ctx, transconjugants selected by cefotaxime.

2.8. Nucleotide sequence accession numbers

Nucleotide sequence data of integrons InK9AT and InK27AT are available in the DDBJ/EMBL/GenBank databases under the accession numbers AB469045 and AB469046, respectively.

3. Results and discussion

The phenotypic tests revealed that 46 *E. coli* and 27 *K. oxytoca* oxyimino-cephalosporin-resistant clinical isolates produced ESBLs. Only one *K. oxytoca* isolate appeared to produce an MBL. Of these β-lactamase producers, 28 *E. coli* and 16 *K. oxytoca* isolates showed resistance to ciprofloxacin and 18 *E. coli* and 12 *K. oxytoca* isolates showed susceptibility to ciprofloxacin.

The bla_{CTX-M} gene was amplified by PCR in 60 (82.2%) of the 73 ESBL producers, including the combination of bla_{TEM} and bla_{CTX-M} in *E. coli* isolates (43.5%; 20/46) and the combination of bla_{SHV} and bla_{CTX-M} in *K. oxytoca* isolates (44.4%; 12/27). The bla_{IMP} gene was detected in one MBL-producing *K. oxytoca* isolate. The bla_{VIM} gene was not observed, and no *bla* genes were detected in five *E. coli* isolates.

For the PMQR genes, *qnrA* was detected in 3 (6.5%) of 46 *E. coli* and 5 (18.5%) of 27 *K. oxytoca* isolates that produced ESBLs, and *qnrB* was detected in 1 *K. oxytoca* isolate producing MBL. The presence of *qnrS* was not observed. The sequences of *qnrA* and *qnrB* were identical to those of *qnrA1* and *qnrB6*, respectively. Of the nine *qnr*-positive isolates, one *E. coli* isolate E5 demonstrated higher resistance to ciprofloxacin (MIC > 64 mg/L), whereas the other eight isolates were susceptible to ciprofloxacin (MIC ≤ 0.5 or 1 mg/L) (Table 1).

The *aac(6′)-Ib-cr* gene was detected in 6 *E. coli* isolates (13.0%) that were resistant to ciprofloxacin (MIC > 64 mg/L), but was not detected in any *K. oxytoca* isolate. These six isolates were positive for bla_{CTX-M}, including two isolates also positive for bla_{TEM}, and this is the first report of *aac(6′)-Ib-cr* identified from the clinical setting in Japan. No isolates possessing *qnr* and *aac(6′)-Ib-cr* in combination were present, suggesting that these two genes have no relationship as described previously in Enterobacteriaceae from the USA [13].

The presence of the *aac(6′)-Ib* gene, responsible for resistance to amikacin, was confirmed in 4 of 9 *qnr*-positive isolates and 1 of 65 *qnr*-negative isolates (amikacin MIC range 8–32 mg/L). The *aac(6′)-IIc* gene, responsible for resistance to gentamicin, was detected in 6 *K. oxytoca* isolates (gentamicin MIC range 4–8 mg/L, except for ≤1 mg/L in isolate K27), comprising 5 of 9 *qnr*-positive isolates and 1 of 65 *qnr*-negative isolates. In the present study, the observation of the *aac(6′)-IIc* cassette prompted us to screen all the isolates for this gene. The results demonstrated that the *aac(6′)-IIc* gene was more prevalent among *qnr*-positive *K. oxytoca* isolates than among all *qnr*-negative isolates (5 of 6 isolates versus 1 of 65 isolates), whilst the *aac(6′)-IIc* gene has been uncommon worldwide, especially in Asia.

All *qnr*-positive isolates possessed combinations of three or more antibiotic resistance genes responsible for resistance to β-lactams, quinolones or aminoglycosides (Table 1). Six isolates carried the $bla_{CTX-M-9}$ ESBL gene, of which five isolates also carried bla_{TEM-1} encoding narrow-spectrum β-lactamase (cefotaxime MIC range 4–16 mg/L). Two *E. coli* isolates harboured the bla_{SHV-12} ESBL gene (ceftazidime MIC > 64 mg/L). The bla_{IMP} allele detected in one phenotypically MBL-positive isolate was identified as bla_{IMP-1}, conferring reduced susceptibility to imipenem and meropenem (MICs 2 mg/L and 4 mg/L, respectively).

The *qnr* genes were transferred from seven clinical isolates (E5, E15, E18, K9, K10, K16, and K27) to their transconjugants (Table 1). The *qnr*-containing transconjugants (K9TC-ctx, K10TC-ctx and K27TC-ctx selected by cefotaxime, and E5TC-cip, E15TC-cip, E18TC-cip and K16TC-cip selected by ciprofloxacin) conferred decreased susceptibility to ciprofloxacin (MIC range 0.125–0.25 mg/L) and levofloxacin (MIC range 0.125–0.25 mg/L), representing 8–16-fold and 4–8-fold increases compared with those of the recipient (MICs of 0.016 mg/L and 0.032 mg/L), respectively. Resistance or reduced susceptibility to β-lactams and aminoglycosides was co-transferred with the *bla* genes and the *aac(6′)* genes carried by donors, respectively. Two *qnr*-negative transconjugants were selected using cefotaxime; bla_{TEM-1}, $bla_{CTX-M-9}$ and *aac(6′)-IIc* were transferred to K5TC-ctx, and bla_{TEM-1} and $bla_{CTX-M-9}$ were transferred to K16TC-ctx. Single plasmids were transferred with or without *qnr* to all transconjugants and their sizes were estimated to be ca. 140 kb. Of these, two representative plasmids in K9TC-ctx and K27TC-ctx were designated pK9AT and pK27AT, respectively.

In the present study, β-lactamase producers frequently possessed the PMQR determinants (20.3%), the AAC(6′) genes (14.9%) or both (12.2%). Further striking features of the present study are the first findings showing that *qnrB6* was carried by an IMP-1 MBL-producing *K. oxytoca* isolate on the same plasmid, and that *qnr*-positive isolates also carried either *aac(6′)-Ib* or *aac(6′)-IIc* on the same plasmid. On the other hand, the linkage of IMP-1 and *qnrB2* in Taiwan [6] and the linkage of VIM-1, *qnrS1* and *aac(6′)-Ib* in Italy [7] have been reported. Our results demonstrating that *aac(6′)-Ib* and *aac(6′)-IIc* were predominant in *qnr*-positive isolates (100%; 9/9) compared with *qnr*-negative isolates (3.1%; 2/65) suggest the genetically close association of quinolone resistance with aminoglycoside resistance.

qnr-positive isolates and their transconjugants carried several types of gene cassettes between 5′-CS and 3′-CS1 (Table 1), and *qnrA1* was located between *orf513* and *ampR*. The complex class 1 integron structure on the plasmids from two *E. coli* isolates was identical to that of In36 (GenBank accession no. AY259085) containing the *dfr16* cassette followed by the *aadA2* cassette.

The structure containing the *aadB* cassette located upstream of the *aadA2* cassette, observed on plasmids from one *E. coli* and four *K. oxytoca* isolates, was similar to that of InKp760 (GenBank accession no. AJ971341), with the replacement of *ampC* with *qnrA1*.

Furthermore, two unique class 1 integrons were found on pK9AT and pK27AT, designated InK9AT and InK27AT, respectively. InK9AT was a novel complex class 1 integron that contained the *aac(6′)-IIc* cassette followed by the *aadA2* cassette, whose structure was also similar to In36 with the replacement of the *dfr16* cassette with the *aac(6′)-IIc* cassette. On the other hand, the bla_{IMP-1} cassette was inserted upstream of the *aac(6′)-IIc* cassette in InK27AT. This structure was similar to In87 (GenBank accession no. AY648125) carrying the bla_{VIM-1} cassette followed by the *aac(6′)-IIc* cassette. The InK9AT cassette arrangement is described for the first time in the present study and we have shown the first identification of the InK27AT cassette arrangement from a *K. oxytoca* clinical isolate and its linkage of *qnrB6* on a single plasmid.

From two unique integrons, two versions of the P_c promoter (formerly P_{ant} or P1) responsible for expression of cassette genes were found in 5′-CS, which were the strong version of P_c (TTGACA–17 bp–TAAACT) found in InK9AT and the weak version of P_c (TGGACA–17 bp–TAAGCT) found in InK27AT. A potential secondary promoter P2 was inactive (TTGTTA–14 bp–TACAGT) in both integrons, although P2 potentially becomes a strong promoter due to insertion of 3 bp into the spacer region. These observations strongly suggest that the different levels of resistance to gentamicin in our transconjugant strains carrying pK9AT and pK27AT (MIC > 8 mg/L for pK9AT versus MIC ≤ 1 mg/L for pK27AT) are affected by different levels of *aac(6′)-IIc* expression owing to the different versions of P_c promoters or the position of the cassette.

The genetic context of *qnrA1* (*orf513–qnrA1–ampR–qacEΔ1*) was conserved among all *qnrA1*-carrying plasmids and was identical to that of In36 and that described in Japan [3], although repeated

attempts to amplify the surrounding regions of *qnrB6* on pK27AT were unsuccessful. In contrast, the cassette content and order within the variable region between 5′-CS and 3′-CS1 on all *qnr*-carrying plasmids have variety. These observations suggest that *qnr*-carrying plasmids have been disseminated with the conserved ISCR1 element and have acquired genetic variety by IntI1-mediated mobilisation of the gene cassettes.

In conclusion, the present study demonstrated the relatively high prevalence of PMQR determinants among ESBL- or MBL-producing isolates in Japan, and two unique integrons were identified on the plasmid carrying the *qnr* genes. Moreover, identification of *qnrB6* and *aac(6′)-Ib-cr*, and close association of *qnr* with *aac(6′)-Ib* and *aac(6′)-IIc*, are described for the first time in clinical isolates producing ESBL or MBL in Japan. The emergence of integrons with novel gene cassettes and plasmid-mediated resistance genes as well as the spread of ISCR1 elements are serious considerations in further dissemination of various resistance genes.

Acknowledgments

The authors thank N. Tajitsu and M. Sakoda for technical assistance in this study.

Funding: The research activity of RS was supported by Grants-in-Aid for Scientific Research from the Japan Society for the Promotion of Science (grant 20930009).

Competing interests: None declared.

Ethical approval: Not required.

References

[1] Robicsek A, Jacoby GA, Hooper DC. The worldwide emergence of plasmid-mediated quinolone resistance. Lancet Infect Dis 2006;6:629–40.

[2] Hata M, Suzuki M, Matsumoto M, Takahashi M, Sato K, Ibe S, et al. Cloning of a novel gene for quinolone resistance from a transferable plasmid in *Shigella flexneri* 2b. Antimicrob Agents Chemother 2005;49:801–3.

[3] Saga T, Akasaka T, Takase H, Tanaka M, Sato K, Kaku M. First detection of the plasmid-mediated quinolone resistance determinant *qnrA* in Enterobacteriaceae clinical isolates in Japan. Int J Antimicrob Agents 2007;29:738–9.

[4] Saito R, Kumita W, Sato K, Chida T, Okamura N, Moriya K, et al. Detection of plasmid-mediated quinolone resistance associated with *qnrA* in an *Escherichia coli* clinical isolate producing CTX-M-9 β-lactamase in Japan. Int J Antimicrob Agents 2007;29:600–2.

[5] Yamane K, Wachino J, Suzuki S, Arakawa Y. Plasmid-mediated *qepA* gene among *Escherichia coli* clinical isolates from Japan. Antimicrob Agents Chemother 2008;52:1564–6.

[6] Wu JJ, Ko WC, Tsai SH, Yan JJ. Prevalence of plasmid-mediated quinolone resistance determinants QnrA, QnrB, and QnrS among clinical isolates of *Enterobacter cloacae* in a Taiwanese hospital. Antimicrob Agents Chemother 2007;51:1223–7.

[7] Aschbacher R, Doumith M, Livermore DM, Larcher C, Woodford N. Linkage of acquired quinolone resistance (*qnrS1*) and metallo-β-lactamase (bla_{VIM-1}) genes in multiple species of Enterobacteriaceae from Bolzano, Italy. J Antimicrob Chemother 2008;61:515–23.

[8] Clinical and Laboratory Standards Institute. Performance standards for antimicrobial susceptibility testing. Fifteenth informational supplement. Document M100-S15. Wayne, PA: CLSI; 2005.

[9] Yagi T, Kurokawa H, Shibata N, Shibayama K, Arakawa Y. A preliminary survey of extended-spectrum β-lactamases (ESBLs) in clinical isolates of *Klebsiella pneumoniae* and *Escherichia coli* in Japan. FEMS Microbiol Lett 2000;184:53–6.

[10] Saladin M, Cao VT, Lambert T, Donay JL, Herrmann JL, Ould-Hocine Z, et al. Diversity of CTX-M β-lactamases and their promoter regions from Enterobacteriaceae isolated in three Parisian hospitals. FEMS Microbiol Lett 2002;209:161–8.

[11] Shibata N, Doi Y, Yamane K, Yagi T, Kurokawa H, Shibayama K, et al. PCR typing of genetic determinants for metallo-β-lactamases and integrases carried by Gram-negative bacteria isolated in Japan, with focus on the class 3 integron. J Clin Microbiol 2003;41:5407–13.

[12] Robicsek A, Strahilevitz J, Sahm DF, Jacoby GA, Hooper DC. *qnr* prevalence in ceftazidime-resistant Enterobacteriaceae isolates from the United States. Antimicrob Agents Chemother 2006;50:2872–4.

[13] Park CH, Robicsek A, Jacoby GA, Sahm D, Hooper DC. Prevalence in the United States of *aac(6′)-Ib-cr* encoding a ciprofloxacin-modifying enzyme. Antimicrob Agents Chemother 2006;50:3953–5.

[14] Cambau E, Lascols C, Sougakoff W, Bébéar C, Bonnet R, Cavallo JD, et al. Occurrence of *qnrA*-positive clinical isolates in French teaching hospitals during 2002–2005. Clin Microbiol Infect 2006;12:1013–20.

[15] Lévesque C, Piché L, Larose C, Roy PH. PCR mapping of integrons reveals several novel combinations of resistance genes. Antimicrob Agents Chemother 1995;39:185–91.

Proteomics Analysis of Mitochondrial Proteins Reveals Overexpression of a Mitochondrial Protein Chaperon, Prohibitin, in Cells Expressing Hepatitis C Virus Core Protein

Takeya Tsutsumi,[1] Mami Matsuda,[2] Hideki Aizaki,[2] Kyoji Moriya,[1] Hideyuki Miyoshi,[1] Hajime Fujie,[1] Yoshizumi Shintani,[1] Hiroshi Yotsuyanagi,[1] Tatsuo Miyamura,[2] Tetsuro Suzuki,[2] and Kazuhiko Koike[1]

The hepatitis C virus (HCV) core protein is involved in viral pathogenesis such as oxidative stress induction and lipid metabolism disturbance, and is primarily located in the cytoplasm and endoplasmic reticulum in association with lipid droplets as well as in the mitochondria. To clarify the impact of the core protein on mitochondria, we analyzed the expression pattern of mitochondrial proteins in core protein-expressing cells by two-dimensional polyacrylamide gel electrophoresis. Several proteins related to the mitochondrial respiratory chain or protein chaperons were identified by mass spectrometry. Among the identified proteins with consistently different expressions, prohibitin, a mitochondrial protein chaperon, was up-regulated not only in core-expressing cells but also in full-genomic replicon cells and livers of core-gene transgenic mice. The stability of prohibitin was increased through interaction with the core protein. Further analysis demonstrated that interaction of prohibitin with mitochondrial DNA-encoded subunits of cytochrome c oxidase (COX) was disturbed by the core protein, resulting in a significant decrease in COX activity. *Conclusion:* The HCV core protein affects the steady-state levels of a subset of mitochondrial proteins including prohibitin, which may lead to an impaired function of the mitochondrial respiratory chain with the overproduction of oxidative stress. (HEPATOLOGY 2009;50:378-386.)

The hepatitis C virus (HCV) is a causative agent of chronic hepatitis, which often leads to cirrhosis and, eventually, to the development of hepatocellular carcinoma (HCC). However, the mechanism of hepatocarcinogenesis in HCV infection is not yet fully elucidated. The HCV core protein forms the viral nucleocapsid protein and has various properties that modulate cellular processes in numerous ways. The core protein binds to cellular proteins, suppresses or enhances apoptosis, and modulates the transcription of some host genes.[1] In addition, transgenic mice expressing the core protein develop HCC,[2-4] indicating a direct contribution of the core protein to the pathogenesis of hepatitis C.

The core protein is mostly localized to the endoplasmic reticulum (ER), but we and other groups have shown its localization to the mitochondria in cultured cells and transgenic mice.[2,5,6] In addition, the double structure of mitochondrial membranes is disrupted in hepatocytes of core-gene transgenic mice.[2-4] Evidence suggests that the core protein modulates some mitochondrial functions, including fatty acid β-oxidation, the impairment of which may induce lipid abnormalities and hepatic steatosis. In addition, the mitochondrion is an important source of reactive oxygen species (ROS). In livers of transgenic

Abbreviations: 2D-PAGE, two-dimensional polyacrylamide gel electrophoresis; COX, cytochrome c oxidase; ER, endoplasmic reticulum; Ero1, ER protein endoplasmic oxidoreduction-1; HCC, hepatocellular carcinoma; HCV, hepatitis C virus; HSP, heat shock protein; IFN, interferon; MnSOD, manganese superoxide dismutase; NS, nonstructural; OST48, oligosaccharyltransferases-48; PDH, pyruvate dehydrogenase; PDI, protein disulfide isomerase; ROS, reactive oxygen species; TFA, trifluoroacetic acid.

From the [1]Department of Internal Medicine, Graduate School of Medicine, University of Tokyo; [2]Department of Virology II, National Institute of Infectious Diseases, Tokyo, Japan.

Received June 17, 2008; accepted March 20, 2009.

Supported by a grant-in-aid for Scientific Research from the Japan Society for the Promotion of Science, from the Ministry of Health, Labour and Welfare of Japan (Research on Hepatitis), from the Ministry of Education, Culture, Sports, Science and Technology (Priority Area), from The Sankyo Foundation of Life Science, and from The Charitable Trust Araki Memorial Promotion Fund. T.T. is an awardee of the Research Resident Fellowship from the Viral Hepatitis Research Foundation of Japan.

Address reprint requests to: Kazuhiko Koike, M.D., Ph.D., Department of Gastroenterology, Internal Medicine, Graduate School of Medicine, University of Tokyo, 7-3-1 Hongo, Bunkyo-ku, Tokyo 113-8655, Japan. E-mail: kkoike-tky@umin.ac.jp; fax: (81) 3-5800-8799

Published online in Wiley InterScience (www.interscience.wiley.com).

DOI 10.1002/hep.22998

Potential conflict of interest: Nothing to report.

Additional Supporting Information may be found in the online version of this article.

mice harboring the core gene, increased ROS production has been observed.[7-9] A recent study found, by the proteomic profiling of biopsy specimens, that an impairment in key mitochondrial processes, including fatty acid oxidation and oxidative phosphorylation, and in the response to oxidative stress occurs in HCV-infected human liver with advanced fibrosis.[10] Therefore, it is probable that the HCV core protein affects mitochondrial functions because such pathogenesis is observed in both HCV core-transgenic mice and HCV-infected patients.[11-13]

The recent progress in proteomics has opened new avenues for disease-related biomarker discovery. Among proteomics approaches, two-dimensional polyacrylamide gel electrophoresis (2D-PAGE) is a technique for the separation and identification of proteins in a sample by displacement in two dimensions oriented at right angles to one another. This method is generally used as a component of proteomics and is the step used for the isolation of proteins for further characterization by mass spectrometry. 2D-PAGE is particularly useful when comparing two related samples such as healthy and diseased tissue. For example, proteins that are more abundant in diseased tissue may represent novel drug targets or diagnostic markers. In fact, several candidate biomarkers for many human cancers have been identified by this approach.[14] There are, however, tens of thousands of proteins in a cell, differing in abundance over six orders of magnitude. 2D-PAGE is not sensitive enough to detect rare proteins, and hence many proteins are not resolved. Therefore, splitting a sample into different fractions is often necessary to reduce the complexity of protein mixtures prior to 2D-PAGE. For this advantage, Lescuyer et al.[15] performed a 2D-PAGE of human mitochondrial proteins derived from the placenta and identified proteins mainly by peptide mass fingerprinting.

In this study, we performed a 2D-PAGE of mitochondria isolated from HepG2 cells stably expressing the HCV core protein and identified several proteins of different expressions when compared with control HepG2 cells. Among up-regulated proteins in the core-expressing cells, we focused on prohibitin, which functions as a mitochondrial protein chaperon, and found that the core protein interacts with prohibitin and represses the interaction between prohibitin and subunit proteins of cytochrome c oxidase (COX), which may lead to decreases in the expression level of the proteins and in COX activity. These results may explain the pathogenesis of liver disease in HCV infection including ROS induction.

Materials and Methods

Cells and Purification of Mitochondria. Hep39 cells,[16] which stably express the HCV core protein, and control HepG2 cells (Hepswx) were grown in Dulbecco's modified Eagle medium (DMEM) containing 10% fetal bovine serum and 1 mg/mL G418. Mitochondria were purified using Nycodenz (Nycomed Pharma, Zürich, Switzerland) according to the protocols reported by Okado-Matsumoto et al.[17] For transient transfection experiments, HepG2 cells were transfected with a core-expression plasmid using TransIT-LT1 (Mirus Bio, Madison, WI). Huh7 cells harboring HCV genotype 1b full-genomic (RCYM1)[18] or subgenomic replicon (5-15), and livers of 3-month-old core-gene transgenic mice[2] were also used for the analysis.

2D-PAGE. Gel electrophoresis in the first dimension was performed using an immobilized pH gradient gel (Immobiline Dry Strip gel, pH 4-7 linear, 13 cm; GE Healthcare, Uppsala, Sweden). The two-dimensional separation was performed on 12.5%, 14 × 16 cm^2, SDS polyacrylamide gels. After the electrophoresis, gels were silver-stained using a silver staining kit (GE Healthcare) according to the manufacturer's protocols. The stained gels were scanned and electronic images of the gels were analyzed using ImageMaster 2D Elite software (GE Healthcare).

In-Gel Digestion and Matrix-Assisted Laser Desorption Ionization, Time-of-Flight Mass Spectrometry (MALDI-TOF-MS). Protein spots on the gels were excised and a "control" piece was cut from a blank region of the gel and processed in parallel with the sample. In-gel digestion with trypsin was performed as reported.[19] The resulting peptides were concentrated using Zip-Tip C18 (Millipore, Bedford, MA). The peptide mixtures were eluted from Zip-Tip with 75% acetonitrile in 0.1% trifluoroacetic acid (TFA). The matrix (α-cyano-4-hydroxycinnamic acid dissolved in 50% acetonitrile, 0.1% TFA) was deposited on a dried sample target. Then 0.5-μL aliquots of the analyte solution were deposited onto matrix surfaces and the solvent was allowed to evaporate at ambient temperature. The digests were analyzed with a TOF mass spectrometer, PE Biosystems Voyager DE STR MALDI (Foster City, CA).

Database Analysis. For protein identification the measured monoisotopic masses of the peptides were analyzed using MS-Fit provided by UCSF (http://prospector.ucsf.edu/ucsfhtml3.2/msfit.htm).

Immunoblotting and Immunoprecipitation. Purified mitochondria were lysed and sonicated in RIPA buffer, then centrifuged at 16,000 rpm for 10 minutes. Protein concentration was determined using a BCA Protein Assay Reagent Kit (Pierce Biotechnology, Rockford, IL). The samples were separated by sodium dodecyl sulfate (SDS)-PAGE and electrotransferred onto a polyvinylidene fluoride membrane (Immobilon; Millipore, Japan), then blocked with BlockAce (Snow Brand, To-

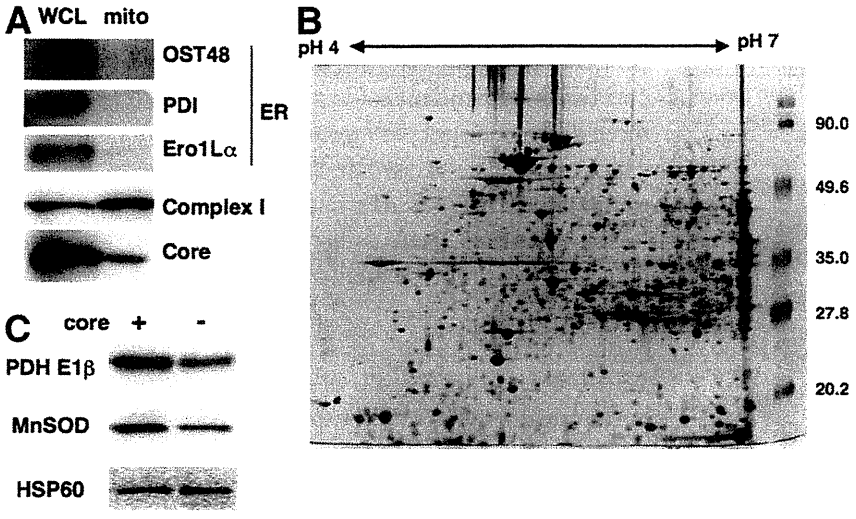

Fig. 1. 2D-PAGE of mitochondria purified from core-expressing cells. (A) Whole-cell lysates (WCL) and purified mitochondria (mito) derived from core-expressing cells were subjected to SDS-PAGE and immunoblotted with anti-core, anti-subunit of complex I (mitochondrial protein), or anti-OST48, PDI, Ero1La (ER proteins) antibodies. (B) Purified mitochondria of core-expressing cells were subjected to 2D-PAGE and the gel was stained with silver. The numbers shown on the right are molecular weights. (C) Purified mitochondria of core-expressing and control cells were subjected to SDS-PAGE and blotted with an anti-E1β subunit of PDH (PDH E1β), anti-MnSOD, or anti-HSP60 antibody.

kyo, Japan). The membrane was subsequently incubated with specific primary antibodies followed by horseradish peroxidase-conjugated secondary antibodies and visualized using SuperSignal West Pico Chemiluminescent Substrate (Pierce). Antibodies against the core protein (Anogen, Mississauga, Canada), manganese superoxide dismutase (MnSOD) (BD Biosciences, San Jose, CA), prohibitin (Neomarkers, Fremont, CA), oligosaccharyltransferase-48 (OST48), heat shock protein (HSP) 60 (Santa-Cruz Biotechnology, Santa Cruz, CA), pyruvate dehydrogenase (PDH), ubiquinol-cytochrome c oxidoreductase, COX (Molecular Probes, Eugene, OR), protein disulfide isomerase (PDI), ER protein endoplasmic oxidoreduction-1 (Ero1)-Lα, and IκBα (Cell Signaling Technology, Danvers, MA), were used as primary antibodies. For immunoprecipitation experiments, cells were lysed in NET-N buffer (20 mM Tris-HCl [pH 8.0], 100 mM NaCl, 1 mM EDTA, 0.5% Nonidet P-40) and the lysates were incubated with anti-prohibitin overnight followed by the addition of protein Sepharose 4B (GE Healthcare), then washed with the same buffer five times. Immunoprecipitates were subjected to SDS-PAGE followed by immunoblotting with specific antibodies.

Determination of COX Activity. COX activity was determined with a MitoProfile Rapid Microplate Assay Kit (MitoSciences, Eugene, OR) using 10 μg of purified mitochondria. The assay was performed three times independently.

Statistical Analysis. Results are expressed as means $\pm$ SE. The significance of the difference in means was determined by Student's t test or Mann-Whitney's U test.

Results

Presence of HCV Core Protein in Purified Mitochondria. Increasing evidence suggests that the HCV core protein is localized to mitochondria as well as to ER and the nucleus. Therefore, we first investigated whether the core protein is expressed in the mitochondria of core-expressing (Hep39) cells used in this study. We used Nycodenz discontinuous gradients to extract mitochondria as described.[17] In the mitochondria derived from core-expressing HepG2 cells, the core protein was detected by immunoblotting, whereas ER resident proteins such as an ER-specific type I transmembrane protein OST48, ER-resident molecular chaperon PDI, and ER membrane-associated N-glycoprotein Ero1-Lα, were not (Fig. 1A). In this fraction, reduced nicotinamide adenine dinucleotide (NADH)-ubiquinone oxidoreductase, complex I of mitochondrial oxidative phosphorylation system, was more strongly expressed than that in the whole cell. These results indicate that the purified mitochondria fraction was free of ER, and that a portion of the core protein was localized to the mitochondria in core-expressing cells.

Proteomics Analysis of Mitochondria by 2D-PAGE. For proteomics analysis, purified mitochondrial proteins derived from core-expressing cells were subjected to 2D-PAGE followed by silver-staining of the gel. In this study we analyzed only acidic proteins using IPG strips covering pH 4 to pH 7 because the analysis of acidic proteins by 2D-PAGE is relatively easy. The mitochondrial fraction was also extracted from Hepswx, a control cell line resistant to G418 but does not express the core protein, then similarly subjected to 2D-PAGE and used for comparing the expression pattern. We repeated the above procedure (purification of mitochondria, 2D-PAGE, and silver-staining) five times, and confirmed a similar expression pattern in core-expressing cells. The representative gel image is shown in Fig. 1B. ImageMaster 2D Elite software detected about 1100 spots on the silver-stained acidic gel, i.e., at pH 4-7 and Mrs of 20-100 kDa. The number of